In situ study of deformation mechanisms in sputtered free-standing nanocrystalline nickel films

R. Mitra,[a] W-A. Chiou,[b] and J.R. Weertman
Department of Materials Science and Engineering, Northwestern University, Evanston, Illinios 60208

(Received 28 August 2003; accepted 25 November 2003)

Nickel films of 1.5–10-μm thickness, produced by dc magnetron sputtering and with disperse grain size distributions peaking in the 30–60-nm range, were subject to in situ tensile straining in a transmission electron microscope. The deformation was stopped frequently, while keeping the load applied, for transmission electron microscopy observation of the internal structure. Contrast changes occurred in many of the grains between strain increments. Ample evidence was seen of dislocation activity, which appears to be the major mechanism for deformation of the samples. Dislocations were seen in grains as small as 20 nm. Parallel arrays of roughly equally spaced dislocations were observed, spaced about 5–10-nm apart. Intergranular nanovoids were found to form and grow with accompanying strain relief in neighboring grains. The results of the current study are generally consistent with previous in situ investigations and contribute to the understanding of deformation mechanisms in free-standing thin films, which may differ somewhat from those in bulk nanocrystalline materials or in films attached to a substrate.

I. INTRODUCTION

The mechanical behavior of nanocrystalline metals has evoked intense interest in recent years, both because of their high strength and the possibility of new deformation mechanisms coming into operation. Though dislocation activity and the buildup of dislocation networks dominate in metals with grain size in the micrometer or larger regime, molecular dynamics (MD) simulations have indicated that at very small grain sizes (less than approximately 30 nm in Ni), plastic deformation is accommodated mainly in the grain boundaries (GBs).[1] At the smallest grain sizes (<12 nm), the deformation is dominated by GB sliding.[2] At slightly larger grain sizes, the simulations predict that emission of partial dislocations from the boundaries contributes to the deformation.[3,4] It is speculated that at still higher grain sizes, emission of perfect dislocations from the boundaries takes over. However, such dislocations leave little debris to be examined in the transmission electron microscope after unloading, as they probably are absorbed in the boundaries. Recent in situ straining experiments tend to bear out this view of deformation in 10-plus nm grain-size samples,[5–7] although experimental difficulties with grain overlap and the high velocity of the moving dislocations have made observations of dynamic dislocation activity difficult. It is clear that dislocation arrays during straining are seen in grains <100 nm in size. In the current paper, we examine changes that occur in Ni films during straining. The grains in these samples cover a number of size ranges, all in the tens of nanometers.

II. EXPERIMENTAL

Nickel films were processed by dc magnetron sputtering of a 99.99% pure Ni target using a power supply of 200 W and a pulsed dc substrate bias of −100 V or −150 V in 6.0 mTorr argon pressure, while keeping the substrate at room (RT) or liquid nitrogen (LN) temperature. The base pressure of the chamber for all depositions was 1×10^{-7} Torr. A previous investigation[8] showed that optimum density and surface smoothness were obtained in 1.5–8-μm-thick Ni films, deposited at either RT or LN temperature, with a substrate bias of −100 V or −150 V. Application of a pulsed dc substrate bias is responsible for argon ion bombardment or resputtering of the film during deposition, which prevents columnar grain growth and assists in the densification of the film but probably results in some trapping of argon. During room temperature deposition with the application of a substrate bias, the grain size increases because of the energy imparted

[a]Present address: Department of Metallurgical and Materials Engineering, Indian Institute of Technology, Kharagpur, 721 302, West Bengal, India.
[b]Present address: Materials Characterization Center, Department of Chemical Engineering and Materials Science, University of California at Irvine, Irvine, CA 92697.
DOI: 10.1557/JMR.2004.0134

by resputtering. Cooling the substrate by liquid nitrogen restricts diffusion during deposition, which prevents grain growth and also increases the nuclei density by reducing the critical radius for nucleation. The details of processing have been published elsewhere.[8] The substrate used was a flat 304-grade stainless steel tensile specimen that was polished using diamond paste up to 1-μm grade and subsequently subjected to ultrasonic cleaning in acetone, followed by methanol or isopropanol. The stainless steel substrate was then coated with 0.25-μm-thick layer of Ni, followed by a 1-μm-thick layer of Cu, using electron beam evaporation. The purpose of the deposition of a buffer layer of Ni was to ensure good adhesion between Cu and the stainless steel. The Ni films for in situ straining studies were deposited on top of the Cu layer. Ni films also were grown on polished and cleaned M2 steel or Si[100] substrates for the purpose of thickness and hardness measurements. Free-standing Ni films were obtained by dissolving the Cu interlayer in a 1 N ferric nitrate solution. The RT film was grown using a −150 V bias and was 1.5-μm thick (film "I"). The two LN films were grown at −100 V bias, 5-μm thick (film "II") and at −150 V bias, 10.0-μm thick (film "III"). Specimens having dimensions of 8.5 mm × 2.5 mm were cut with a sharp razor blade from the free-standing films. Subsequently, holes were punched at the ends for the purpose of attaching the sample to the grips of the transmission electron microscope specimen holder. The distance between the screws was 6 mm, which is considered as the nominal gauge length in this study. For transmission electron microscopy (TEM) examination, a 3-mm-diameter region in the center of the films was argon ion-milled on a Gatan Inc. (Pleasanton, CA) ion-mill (model 600) using the standard liquid nitrogen–cooled holder. Ion-milling time varied between 40 min and 2 h, depending on the thickness of the film. TEM studies were performed on a Hitachi (Pleasanton, CA) 8100 transmission electron microscope at an accelerating voltage of 200 kV. A Gatan single tilt straining holder (model 654) was used for the in situ deformation. The elongation rate during the straining was 0.1 μm/s, which would be equivalent to a strain rate of 1.7×10^{-5}/s if the elongation were uniform. Regions up to a distance of about 10 to 30 grains away from the edge of the central hole were examined, although in one case (Fig. 4), the viewing was only about five grains away. The holes appeared smooth and did not seem to lead to crack initiation under deformation. Because the region around the hole in each of the specimens was thinned, strain-localization occurred here, leading to a higher strain rate in this area. For observation during deformation, slightly thicker regions with few small holes or pores were chosen. Micrographs of a specific region were recorded at intervals of a few micrometers displacement, while the specimen was under load, without any change in the tilt of the specimen The time interval between stopping at a particular displacement and recording a micrograph was roughly between 0.5 and 1 min, which included the time to fine focus, briefly observe the microstructure, and expose the film. A thorough study of the deformation of the grains of different size ranges and shapes has been carried out, with emphasis on the relatively smaller grains in the microstructure. The micrographs discussed represent the general trend observed in the samples.

III. RESULTS

A. Grain size distributions and microstructures

The specimens obtained from films I, II, and III follow the same naming system. Figure 1 shows the grain size distributions of the three films plotted using a lognormal relationship.[8,9] The size of approximately 200 grains was measured from TEM negatives of each of the films. The modes of grain-size distribution in specimens I, II, and III are 65 nm, 43 nm, and 32 nm, respectively, while the mean grain sizes are 126, 75, and 79 nm, respectively. The average grain size was much smaller in the thinner films, such as those of 100-nm thickness,[8] implying that grain growth took place as the film thickness increased. However handling of thin films becomes more difficult as thickness decreases, and films with less than 1.5-μm thickness could not be used for this reason. The films grown in this study showed a random orientation of the grains.

Micrographs from specimen I are shown in Fig. 2: (a) in the as-deposited, undeformed condition; (b) extension of 7.6 μm; (c) and (d) 24.6 μm; and (e) 30.6 μm. These extensions correspond to strains averaged over the entire sample of 0.13%, 0.4%, and 0.5%, respectively. Figures 3(a) and 3(b) show the low-magnification bright-field images of specimen II in the (a) as-deposited, undeformed condition and (b) after a displacement of 4 μm.

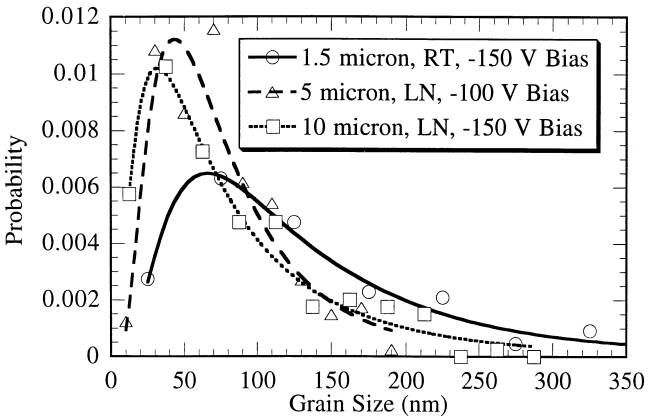

FIG. 1. Lognormal grain size distributions of film I grown at room temperature and films II and III grown at liquid-nitrogen temperature.

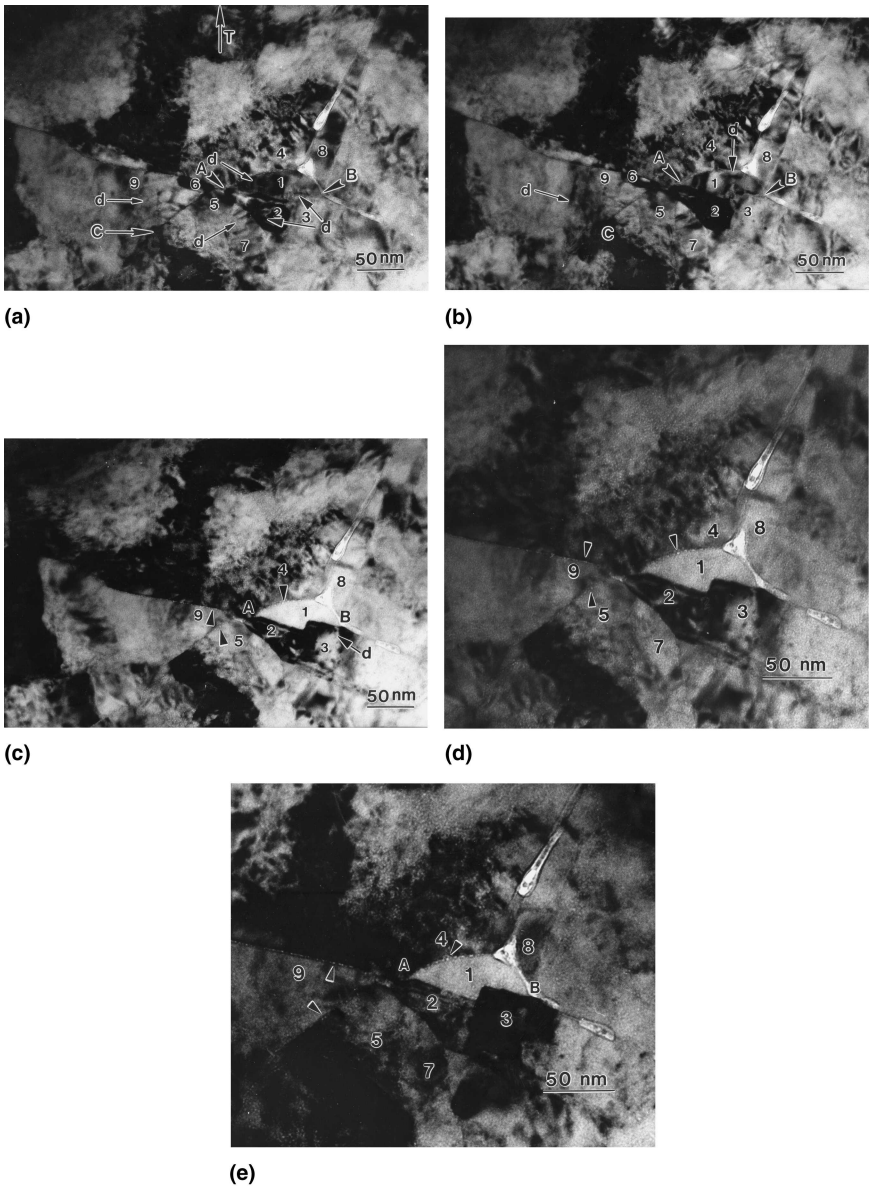

FIG. 2. Bright-field TEM micrographs of film I in (a) undeformed condition and after extension of the specimen by (b) 7.6 μm, (c) 24.6 μm at low magnification, (d) 24.6 μm, and (e) 30.6 μm at higher magnification. Grains "1"–"9" have been identified for comparative study. "A" and "B" are triple point junctions on the boundary of grain "*1*" with neighboring grains. Point "C" is a source for emission of dislocation loops. The arrows marked as "d" in (a) and (b) show dislocations, whereas the arrowheads in (c) and (d) show grain boundaries with a chain of nano-sized voids. "T" represents the direction of the applied strain.

Higher magnifications of a part of Figs. 3(a) and 3(b) are shown in Figs. 3(c)–3(f), corresponding to increasing displacements of 4, 6, 7, and 9 μm; average strains of 0.067%, 0.10%, 0.12%, and 0.15%, respectively. The choice of a pair of low-magnification images is to show the effect of straining over a large area, while we focus our attention on a smaller area of interest for details. Another area of specimen II in undeformed condition and after a displacement of 397 μm has been shown at low magnification in Figs. 4(a) and 4(b), respectively. The stages of specimen II after extensions of 397 μm (6.6% total specimen strain) and 441 μm (7.4% specimen strain) are shown at higher magnification in Figs. 4(c) and 4(d), respectively. Figures 5(a) and 5(b) show low-magnification bright-field TEM images of specimen III in the undeformed condition and then after a displacement of 27 μm, respectively. The stages of extension of specimen III, from a crosshead displacement of 27 μm (0.45% specimen strain) to that of 30 μm (0.5% specimen strain) are shown at higher magnification in Figs. 5(c) and 5(d), respectively. The grains have varying shapes and aspect ratios because of the initial

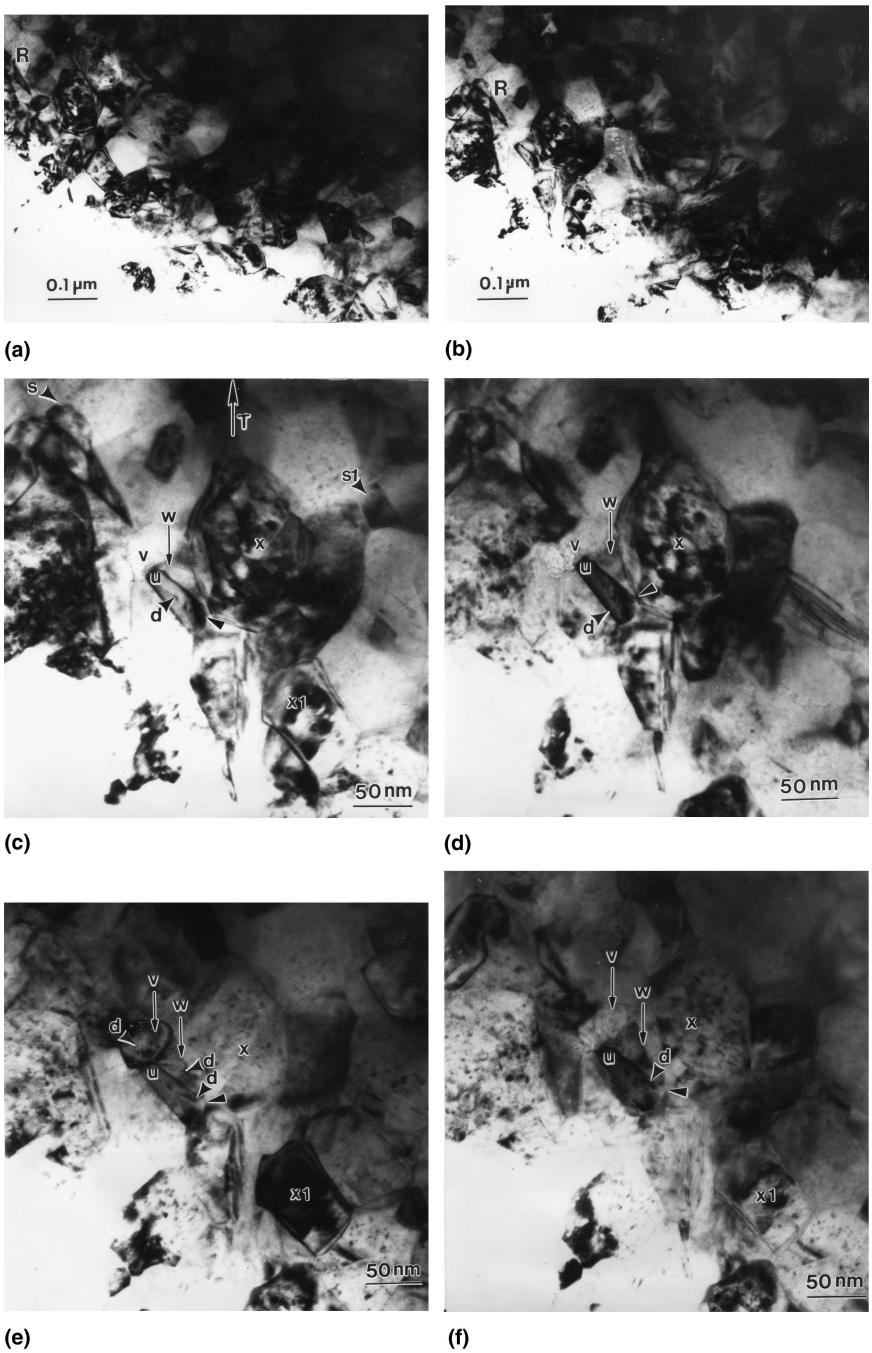

FIG. 3. Bright-field TEM micrographs of film II showing the stages of in situ straining corresponding to elongations of the specimen by (a) 0 μm and (b) 4 μm at low magnification, (c) 4 μm, (d) 6 μm, (e) 7 μm, and (f) 9 μm at higher magnification. "R" is the point of reference to facilitate comparison of the two low-magnification images. Grains "*u*," "*v*," "*w*," "*x*," and "*x1*" are marked for comparison. Arrowheads with straight edges point to the corner of grain "*u*," which comes in point contact with grain "*x*" during straining. Arrowheads, with curved edges and marked as "d," show dislocations. "T" represents the direction of the applied strain.

tendency for columnar growth, which is interrupted by resputtering due to the application of a substrate bias.

B. Nanoindentation hardness

The hardness values of Ni films, each having the same thickness and growth conditions as the corresponding film I, II, or III, were measured by nanoindentation while the films were attached to their M2 steel substrates. After corrections for instrumentation effects, the following hardness values were measured: film I, 4.7 ± 0.2 GPa; film II, 5.0 ± 0.2 GPa; film III, 3.8 ± 0.1 GPa. The depth of indentation was kept between 10 and 15% of the film

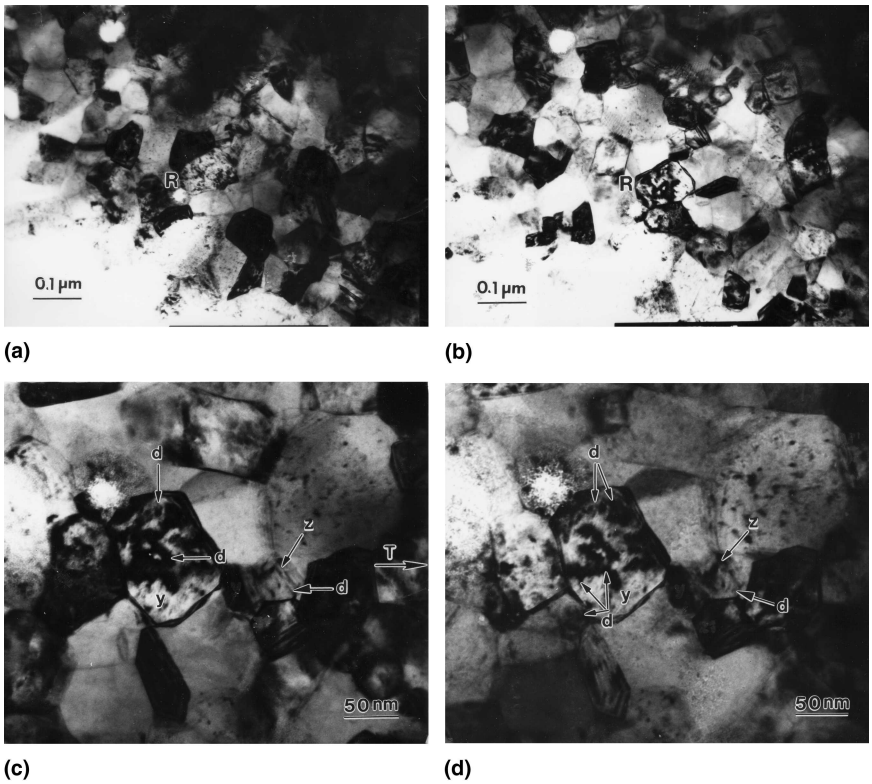

FIG. 4. Bright-field TEM micrographs of film II showing the stages of in situ straining, corresponding to specimen elongations of (a) 0 μm and (b) 397 μm at lower magnification, (c) 397 μm, and (d) 441 μm at higher magnification. "R" is the point of reference to facilitate comparison of low-magnification images. The grains "*y*" and "*z*" are marked. The dislocations in arrays are shown with arrows, marked as "d." "T" represents the direction of the applied strain.

thickness to minimize the effect of the substrate. Measurements could not be carried out on free-standing films because they did not lie flat. The hardness values here do not really scale with the mean grain size. Besides mean grain size, the width of the grain size distribution, the specimen density, and the distribution of pore sizes all affect the hardness. For example, argon entrapment in the films grown at liquid-nitrogen temperature is expected to be significant as a result of resputtering produced by the substrate bias. At a substrate bias of –150 V (as in film III), entrapment of Ar gas atoms is expected to be greater than in case of –100 V bias. On warming up to room temperature, the argon is released, leaving behind pores on the surface. Thus, it can be seen that grain size is not the only factor determining the hardness of these samples.

Nickel films of 1.0-μm thickness grown under the conditions of film I, II, and III experienced a tensile residual stress of about 0.6 GPa while attached to the substrate, as measured by the curvature of the film–substrate combination.[8] This stress is expected to disappear upon release of the film from the substrate. The residual stress is expected to be less in the relatively coarse-grain thicker films as the grains undergo plastic deformation to relieve it. The grains in the as-deposited, free-standing film I of 1.5-μm thickness in Fig. 2(a) show a dislocation structure even before the start of the in situ straining takes place.

C. Deformation behavior

In the current work, the activity of dislocations in the grains of different sizes and shapes has been qualitatively studied in an effort to understand the deformation mechanism(s) producing the observed microstructural changes. As mentioned in the Sec. I, molecular dynamics simulations of nanocrystalline Ni with grain size in the range of approximately 10 to 15 nm under tensile stress indicate that emission of partial dislocations from the GBs contributes to the plastic deformation, and it is believed that at larger grain sizes (probably including the size range in the current experiment), loops of perfect dislocations emanating from the grain boundaries are primarily responsible for the plastic deformation.[3,4] During in situ straining of coarse-grained materials, where the grain size is comparable to the film thickness, the image forces of the free surface and pinning of dislocations by surface oxide layers lead to a deformation behavior different from that of bulk materials. However, in nanocrystalline metals, because the grain size is much finer than the thickness of the TEM specimens, it has been argued that

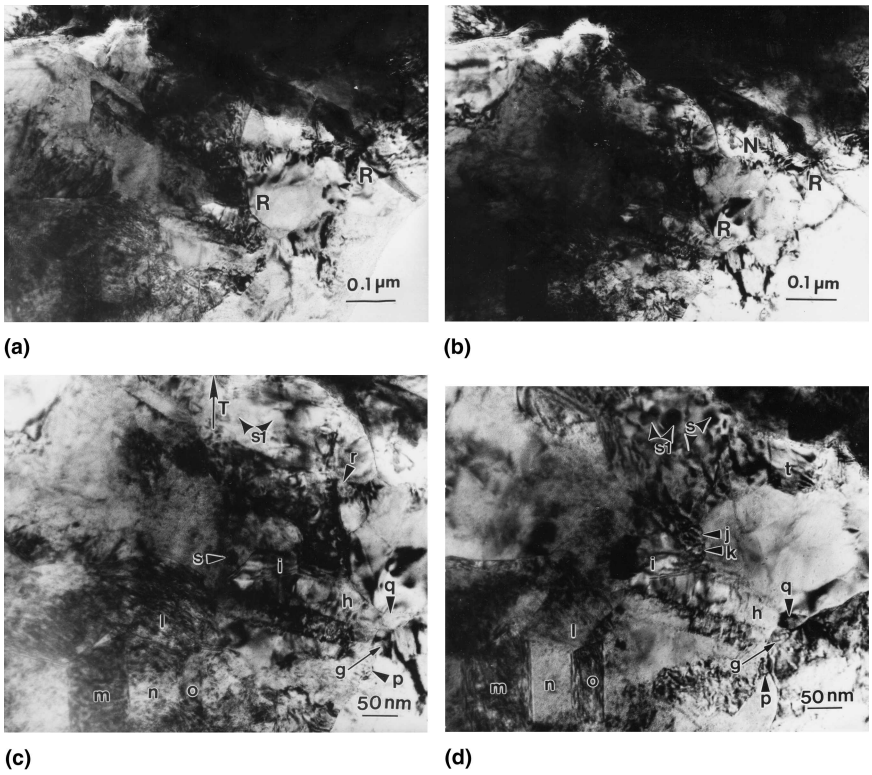

FIG. 5. Bright-field TEM images of specimen III, corresponding to specimen extensions by: (a) 0 μm (low magnification), (b) 27 μm (low magnification), (c) 27 μm (high magnification), and (d) 30 μm (high magnification). "R" is the point of reference to facilitate comparison of low-magnification images. A number of grains are marked with the letters of the sequence "*g*"–"*t*" and "*s1*." The grains "s1," "g," and "q" are marked in (c) in the same position where those appear in (d). "T" represents the direction of the applied strain.

deformation as seen in this case should be much closer to that of the bulk material.[10] Recently, Derlet and Van Swygenhoven[11] have used MD simulations to show that two parallel surfaces have a strong effect on the deformation of thin films, causing increased grain boundary sliding as well as greater dislocation activity. The influence of a free surface diminishes after the outermost grain and becomes small for interior grains. The distorting effect of the free surfaces should be kept in mind when interpreting TEM observations of deformation. However, the grain sizes considered by Derlet and Van Swygenhoven were 5 nm and 12 nm. Thus, a 2-grain thickness in their study would be 24 nm at most, which is much thinner than the foils used in the current study. The experimental observations of deformation behavior are discussed below, with examples.

TEM observations during straining

The study shows that under tensile deformation, the grains, which may or may not show dislocations when viewed during interruptions in the straining, can change contrast sharply on slight extensions. Pronounced contrast changes are obvious from a comparison of corresponding grains in images taken before and after a deformation increment. The contrast changes so sharply that few regions are similar in Figs. 3(a) and 3(b), 4(a) and 4(b), or 5(a) and 5(b). Hence the label "R" has been marked on the low-magnification images, so that corresponding grains can be matched up easily. Strong contrast changes caused by even small extensions may be the result of localized stress peaks arising from strain localization leading to grain rotation, accompanied by dislocation motion. Such rapid changes in contrast were seen in previous in situ straining experiments involving Cu and Ni nanocrystalline samples in which the TEM observations were captured on a video camera operating at 30 frames/s.[5–7] The dislocations moved too quickly to be caught in motion on camera. In the current study, changes in contrast can be seen between successive viewings in a number of grains. Examples of such abrupt changes are grain *v*, which shows strong contrast in Fig. 3(e) but is hardly visible in Figs. 3(c) and 3(d) and is in weak contrast in Fig. 3(f); grains *s* and *s1*, which are evident in Fig. 3(c) but indistinguishable or hardly evident in Figs. 3(d)–3(f); grain x1 is not obvious in Fig. 3(d) but is visible in others of the set; and grains *s1*, *j*, *k*, *q*, *r*, and *t* are visible in either Fig. 5(c) or 5(d) but not easily seen in both. The variation in contrast with increasing strain occurs in grains of all sizes studied in this work. The dislocations are arrowed and marked as

"d" in Figs. 2(a)–2(d), 3(c)–3(f), and 4(c) and 4(d). Examples of the presence of dislocations can be seen in grains *j*, *k*, *r*, and *t* of Fig. 5(c) or 5(d), and grains *1* and *7* in Figs. 2(a) and 2(b). Grain *k* [Fig. 5(d)] appears to be slightly less than 20 nm in size (close to the minimum grain size in the sample, as shown in Fig. 1), and the other grains in Figs. 5(c) and 5(d) mentioned above showing dislocations are in the 25–30-nm range. Arrays of dislocations, parallel and roughly uniformly spaced approximately 5–10 nm apart, can be seen in grain *7* [Fig. 2(a)], grain *z* [Fig. 4 (c)], and grains *j* and *t* [Fig. 5(d)]. Without a video camera it was not possible to tell if these dislocations were moving, as observed by Youngdahl et al.[7] and Kumar et al.[6] in the case of similar arrays, but such motion would account for the rapid contrast changes seen in the video-equipped straining experiments. The arrangement and number of dislocations change with increasing strain, as is observed when the grain "z" of Fig. 4(c) is compared with that of Fig. 4(d). Dislocation loops appear to have emanated from point *C* into grain *9* in Fig. 2(a), but are no longer seen in the rest of Figs. 2(b)–2(d). The external strain has yet to be applied in Fig. 2(a), but it is known that the internal stresses are high when the film is attached to the substrate.[8] A small elongated void, probably a preexisting flaw, is seen between grains *4* and *8* [Figs. 2(a)–2(d)], and a triple-point void lies between grains *4*, *8*, and *1*. As straining proceeds, nanovoids grow on the grain boundary between grains *1* and *4* [barely detectable in Figs. 2(a) and 2(b), larger in Figs. 2(c) and 2(d)]. With the extensive porosity on one grain boundary, plus the presence of the triple point void and the associated crack at B, grain *1* appears to undergo stress relief. Evidence of any dislocation presence in grain *1* is missing from Figs. 2(c) and 2(d). Nanovoids also form on two of the boundaries of grain *9* in the same figures. The formation of these voids may be responsible for the disappearance of much of the dislocation presence in this grain. Figures 2 to 5 offer ample evidence of dislocation networks in grains >100 nm in size. A typical dislocation network is labeled as "N" in Fig. 5(b). Some of the grains, such as "l", "m" "n" and "o" in Figs. 5(c) and 5(d) not only change contrast with increasing strain, but show a high density of dislocations in general.

Dislocation activity can change the orientation of a grain. An example of apparent grain rotation under deformation is shown in Figs. 3(c)–3(f). In the first shot, before straining has started, grains *u* and *x* are separated by about 3 nm, but as straining proceeds, the two grains establish point contact, as seen in Fig. 3(d). The proximity of these grains to the perforation hole may make it easier for the grains to rotate.[10] The mechanism of grain rotation during deformation to accommodate the constraint imposed by continuity across the grain boundary in polycrystalline metals has been discussed by Hirth.[12]

The change in contrast, discussed above, is certainly not due to local bending of specimens. The sharp changes in contrast of entire individual grains [Figs. 3(a), 3(b), 4(a), 4(b)] relative to neighboring grains during straining imply that change in contrast is not due to local bending of the foil. The bent area is unlikely to be confined to just specific randomly oriented grains. The contrast due to bending can be observed inside the group of grains to the right of grain "p" in Fig. 5(c), where the effect is observed across the neighboring grains. It is observed in the thin region, very close to the perforation hole.

The contrast changes occur instantaneously with the progress of straining. Even small increments in strain led to sharp alterations in contrast. No change in contrast with time could be observed in any area during TEM observation of a sample before straining, in-between strain increments, or after completion of the straining. The acceleration voltage of 200 kV did not appear to cause any damage to the specimens during this study in spite of the extended exposure of some of the chosen regions. Of course, studies were conducted with a spread-out beam, by controlling the strength of condenser lens I in a double-condenser system. The high thermal conductivity of Ni, along with the use of a defocused electron beam away from cross-over, small spot size, and acceleration voltage of 200 kV prevented specimen heating. The effect of specimen heating has not been mentioned in previous studies on in situ straining. The thermal conductivity of Ni is high and the thicknesses of the regions studied were around 100–150 nm. In such cases, specimen heating is expected to be negligible. In Ref. 13 it is noted that electron beam-induced effects on dislocation motion in thin foils occur at a specimen thickness less than 2–3 times the extinction distance. The extinction distances of nickel for low index ⟨111⟩ and ⟨200⟩ orientations are between 23.6 nm and 27.5 nm, respectively. It is intuitive to believe that foil thickness is a more important parameter in determining the effect of the electron beam on dislocation motion than the number of grains through the foil thickness. Thus, electron beam-induced rearrangement of dislocations is ruled out.

IV. DISCUSSION

Evidence has been presented in the preceding section for the participation of dislocations in the deformation of the nanocrystalline Ni samples. Dislocations were seen in grains even smaller than 20 nm. These findings are consistent with earlier observations during in situ straining by Youngdahl et al.,[7] Kumar et al.,[6] and Hugo et al.,[5] as well as the results of molecular dynamics simulations.[3,4] Hugo et al. reported the presence of dislocations in grains as small as 10 nm. In the current investigation, arrays of more-or-less parallel dislocations were seen in a number of grains with spacings of 5–10 nm. These dislocations

could not be described as forming "pile-ups" because their spacing was reasonably uniform. Such arrays also were seen in the previous in situ studies[6,7] and in Ref. 7 were observed to be moving across a grain and appeared to be disappearing into a grain boundary. Because a video camera was not available for the current studies, it was not possible to observe the dynamics of the contrast changes as was done in the studies mentioned above. However, the changes in the appearance of grains between strain increments indicate that such dislocation motion was taking place.

In the current study, dislocations, especially in the larger grains, and some very small grain boundary nanovoids were observed in the foils even before straining began. They probably formed during the synthesis process and can be associated with the high internal strains in the films.[8] Observations of the appearance of fresh nanovoids on some grain boundaries and the growth of preexisting voids on other boundaries suggest that fracture is likely to be intergranular, consistent with the observations of Hugo et al.[5]

Recent simulations of crack propagation by Farkas and Van Swygenhoven (unpublished data) have shown that a nanocrystalline sample undergoing tensile straining exhibits enhanced dislocation activity and deformation twinning in the neighborhood of a crack, compared to the behavior of a completely intact sample under similar deformation conditions. Previous experimental in situ straining studies were done in close proximity to cracks,[5–7] whereas in the current case most of the observations were carried out well away from a hole with a rounded perimeter. No evidence was seen for deformation twinning, as was believed to have been observed in Ref. 6.

There is little evidence for a significant contribution to the deformation associated with grain boundary sliding processes leading to grain rotation. This is to be expected given the size of the grains in the current study and is in agreement with the conclusions of Hugo et al.[5] However, in a recent study, Wang and Ma (unpublished data) have shown that a thermally activated deformation process operates at room temperature in Cu samples with grains in the submicrometer-size range. This process is suppressed at liquid-nitrogen temperatures. The authors conclude that the results of their investigation appear "consistent with a grain boundary-related process that can be accommodated at room temperature during slow deformation." It is not clear if this process would apply to the current nickel samples. The change in orientation of grains induced by slip is more likely in the current study.

V. CONCLUSIONS

In situ tensile straining experiments have been carried out on free-standing nanocrystalline Ni films processed by dc magnetron sputtering, with substrates at room or liquid-nitrogen temperature and negatively biased at –100 V or –150 V. The samples contained equiaxed grains with a wide dispersion in grain size, peaking at about 30–60 nm depending on the processing conditions. Straining was carried out with frequent interruptions for observation of the internal structure by TEM, while keeping the samples under load. The results are in general agreement with previous in situ dynamic studies of the deformation of nanocrystalline metals studied by TEM.

(1) Contrast changes were seen in many of the grains between strain increments.

(2) Dislocations were observed in grains as small as 20 nm, which is close to the smallest grain size in the samples. Dislocation networks were present in the large grains.

(3) Dislocation activity appears to play the major role in the deformation of these samples.

(4) Parallel arrays of dislocations, roughly evenly spaced approximately 5–10-nm apart, were seen in a number of grains.

(5) Nanovoids were observed to form on some of the grain boundaries and grow as the straining progressed. They also were seen in some undeformed samples. The nanovoids appeared to lead to strain relaxation.

(6) The current study contributes to the understanding of deformation behavior of free-standing nanocrystalline thin films, which may be somewhat different from bulk behavior.

ACKNOWLEDGMENTS

The contributions of the late Dr. Richard Hoffman of the former Advanced Coating Technology Group of Northwestern University to the preparation of free-standing Ni films are gratefully acknowledged. This research used the Materials Research Center Facilities at Northwestern University, supported by the National Science Foundation under Grant No. DMR-9632742. One of the authors (R.M.) is grateful to the Defense Research and Development Organization, New Delhi, India, for granting leave of absence for pursuing this research. This research was partially supported by the United States Department of Energy under Grant No. DE-FG02-86ER45229.

REFERENCES

1. H. Van Swygenhoven, Polycrystalline materials: Grain Boundaries and Dislocations, Science **296,** 66 (2002).
2. H. Van Swygenhoven and P.M. Derlet, Grain boundary sliding in nanocrystalline fcc metals, Phys. Rev. B **64,** 224105 (2001).
3. H. Van Swygenhoven, P.M. Derlet, and A. Hasnaoui, Atomic mechanism for dislocation emission from nanosized grain boundaries, Phys. Rev. B **66,** 024101 (2002).
4. P.M. Derlet, H. Van Swygenhoven, and A. Hasnaoui, Atomistic

simulation of dislocation emission in nanosized grain boundaries, Philos. Mag. A **83,** 3569 (2003).
5. R.C. Hugo, H. Kung, J.R. Weertman, R. Mitra, J.A. Knapp, and D.M. Follstaedt, In-situ TEM Tensile Testing of DC Magnetron Sputtered and Pulsed Laser Deposited Ni Thin Films, Acta Mater. **51,** 1937 (2003).
6. K.S. Kumar, S. Suresh, M.F. Chisholm, J.A. Horton, and P. Wang, Deformation of electrodeposited nanocrystalline nickel, Acta Mater. **51,** 387 (2003).
7. C.J. Youngdahl, J.R. Weertman, R.C. Hugo, and H.H. Kung, Deformation behavior in nanocrystalline copper, Scr. Mater. **44,** 1478 (2001).
8. R. Mitra, R.A. Hoffman, A. Madan, and J.R. Weertman, Effect of process variables on the structure, residual stress and hardness of sputtered nanocrystalline nickel films, J. Mater. Res. **16,** 1010 (2001).
9. R. Mitra, T. Ungar, T. Morita, P.G. Sanders, and J.R. Weertman, Assessment of grain size distributions in nanocrystalline copper and their effect on mechanical behavior, in *Advanced Materials for the 21st Century: The 1999 Julia R. Weertman Symposium*, edited by Y-W. Chung, D.C. Dunand, P.K. Liaw, and G.B. Olson (TMS, Warrendale, PA, 1999), p. 553.
10. W.W. Milligan, S.A. Hackney, M. Ke, and E.C. Aifantis, In situ studies of deformation and fracture in nanophase materials, Nanostruct. Mater. **2,** 267 (1993).
11. P.M. Derlet and H. Van Swygenhoven, The role played by two parallel free surfaces in the deformation mechanism of nanocrystalline metals: A molecular dynamics simulation, Philos. Mag. A **82,** 1 (2002).
12. J.P. Hirth, The influence of grain boundaries on mechanical properties, Metall. Trans. **3,** 3047 (1972).
13. J.W. Edington, *Practical Electron Microscopy in Materials Science* (Philips, Eindhoven, 1975), p. 9.